DOI: 10.1002/ange.201305061

Drug Delivery

Cucurbit[7]uril Containers for Targeted Delivery of Oxaliplatin to Cancer Cells**

Liping Cao, Gaya Hettiarachchi, Volker Briken, and Lyle Isaacs**

The fundamental molecular recognition properties of the cucurbit[*n*]uril (CB[n]; $n = 5, 6, 7, 8, 10$) family[1] of molecular containers has been widely explored over the past decade.[2] Some of the most useful recognition properties include the extraordinary binding affinity and selectivity of CB[*n*] toward suitable guests (K_a up to $10^{15}\,M^{-1}$),[3] the anomalously low polarizability of the CB[*n*] cavity,[4] the large pK_a shifts experienced by bound guests,[5] the ability of certain CB[*n*] to form ternary host·guest$_2$ complexes,[6] and the stimuli responsiveness (e.g. chemical, photochemical, electrochemical) of the corresponding CB[*n*]·guest complexes.[2] More recently, the focus of research in the CB[*n*] area has shifted toward the preparation of systems with function. For example, the recognition properties of CB[*n*] have been exploited to create chemical sensing ensembles,[7] molecular machines,[6a] supramolecular materials,[8] perform supramolecular catalysis,[9] and solubilize, formulate, and deliver drugs.[10,11]

Oxaliplatin is a platinum anticancer agent that is approved as a first-line chemotherapeutic for the treatment of advanced colorectal carcinoma in combination with other anticancer drugs.[12] However, patients treated with oxaliplatin commonly experience peripheral neuropathy and moderate myelotoxicity in a cumulative dose dependent manner.[12] Accordingly, the development of an improved version of oxaliplatin with an expanded therapeutic window is an urgent need.[12] Previously, Kim, Day, and Wheate et al. reported the encapsulation of the anticancer agent oxaliplatin inside CB[7], its protection against degradation reactions with biological nucleophiles, and its reduced in vitro cellular bioactivity.[13] In recent years, targeted (e.g. folate and RGD) versions of chemotherapeutic drugs have been widely explored with numerous scaffolds (e.g. nanoparticles, liposomes, antibodies, polymers, dendrimers) with the goal of enhancing therapeutic efficacy and reducing side effects.[14] Recently, we and others have developed the first routes to prepare monofunctionalized derivatives of CB[6] and CB[7].[15] As such, we saw an opportunity to prepare a targeted molecular container that features a covalently attached targeting ligand on its convex face and a CB[7] sized cavity to allow it to encapsulate a wide range of drugs and bring them along for the ride.[16] Herein we report the preparation of CB[7] derivative **1** that bears a covalently attached biotin targeting ligand, which results in efficient targeting of **1**·oxaliplatin to L1210FR cells and enhanced in vitro cytotoxicity.[17]

The preparation of biotin-functionalized container **1** begins with an improved preparation of the methylene-bridged glycoluril hexamer that serves as the starting material for CB[7] derivative **2** that bears a primary alkyl chloride functional group (the Supporting Information).[15a,d] We are now able to access **2** in 960 mg batches. Compound **2** is transformed into azide **3** (92%) as described previously[15d] and then reduced to the corresponding amine with triphenylphosphine and isolated as its hydrochloride salt **4** in 93% yield (Scheme 1). Fortunately, the $(CH_2)_4$ linker between the CB[7] ring and the NH_3^+ functional group is too short to allow for cavity inclusion binding (the Supporting Information), thus allowing **4** to function as a good nucleophile in amide bond forming reactions. For example, CB[7] derivative **4** undergoes reaction with biotin *N*-hydroxysuccinimide ester in DMF as solvent to deliver **1**, which features a covalently attached biotin unit, in 78% yield. CB[7] derivative **5** with a longer covalent spacer was prepared similarly in 67% yield.

The ^{1}H NMR spectra recorded for **1** on its own (Figure 1a) is broad and uninterpretable. However, the ^{1}H NMR spectrum of **1** recorded in the presence of *p*-xylene diammonium ion (**6**; Figure 2) as its **1**·**6** complex (Figure 1b) exhibits sharp resonances in the CB regions of the spectrum and diagnostic resonances for the linker-biotin portion of **1**. Our interpretation of this data is that **1**—by virtue of its CB[7] sized cavity and biotin arm—undergoes self-association in water. To determine the oligomerization state of **1** in water we performed diffusion ordered spectroscopy (DOSY) for both **1** and **1**·**6**.[18] The Supporting Information (Figure S18a,b) shows the decay in signal intensity versus the strength of the magnetic field gradient, which can be fitted in the usual way to extract the diffusion coefficients of the species of interest. The 18% decrease in the average diffusion coefficient for **1** ($1.83 \times 10^{-10}\,m^2s^{-1}$) relative to monomeric **1**·**6** ($2.23 \times 10^{-10}\,m^2s^{-1}$) is consistent with the formulation of the solution structure of **1** as the dimer $\mathbf{1}_2$.[18]

In order for **1** to be useful as a container for the targeted delivery of drugs, the dimer $\mathbf{1}_2$ must be easily disassembled in

[*] Dr. L. Cao,[+] Prof. Dr. L. Isaacs
Department of Chemistry and Biochemistry
University of Maryland
College Park, MD 20742 (USA)
E-mail: LIsaacs@umd.edu
G. Hettiarachchi,[+] Prof. Dr. V. Briken
Department of Cell Biology and Molecular Genetics
University of Maryland
College Park, MD 20742 (USA)
E-mail: vbriken@umd.edu
[+] These authors contributed equally to this work.

[**] L.I. thanks the National Science Foundation (CHE-1110911) and V.B. thanks the National Cancer Institute of the NIH (R01 CA168365) for financial support. G.H. thanks the University of Maryland for a Wylie Fellowship.
Supporting information for this article is available on the WWW under http://dx.doi.org/10.1002/anie.201305061.

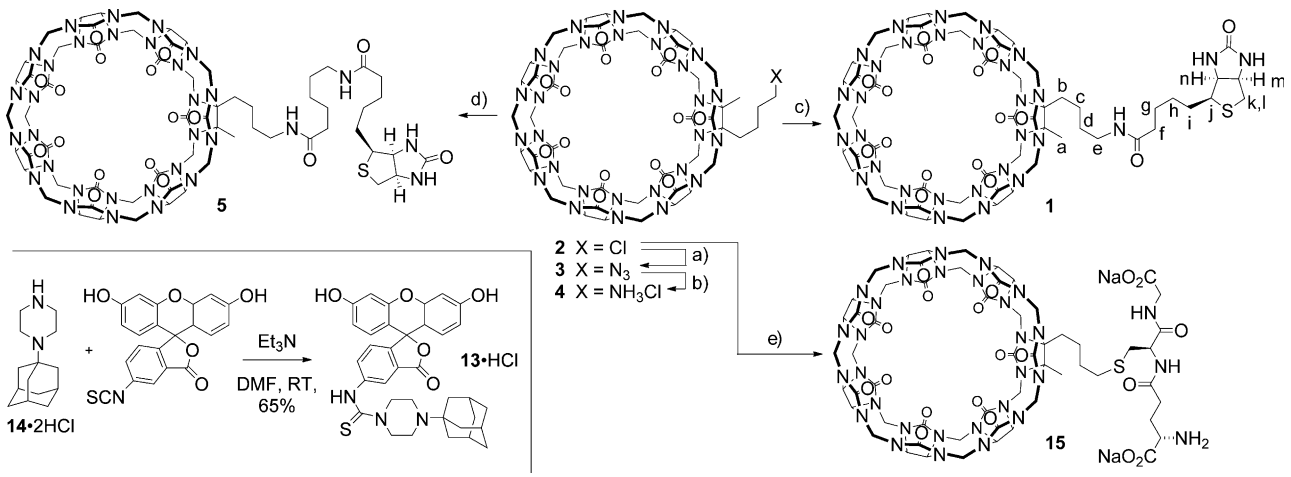

Scheme 1. Synthesis of CB[7] derivatives **1**, **5**, and **15** as well as fluorescent adamantane derivative **13**. Conditions: a) NaN_3, 80 °C, 92 %, b) PPh_3, RT, then 1 M HCl, 93 %, c) biotin-*N*-hydroxysuccinimide ester, Et_3N, 50 °C, 78 %, d) biotinamidohexanoic acid *N*-hydroxysuccinimide ester, Et_3N, 50 °C, 67 %, e) NaI, acetone, reflux, then L-glutathione, NaOH, H_2O, RT, 69 %.

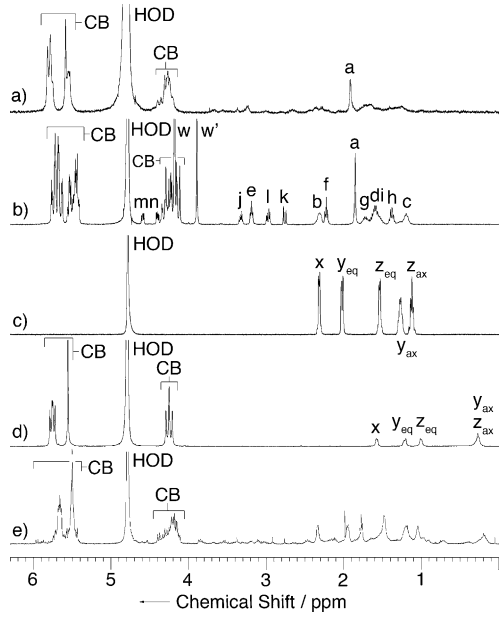

Figure 1. ^{1}H NMR spectra recorded (400 or 600 MHz, D_2O, RT) for: a) $\mathbf{1}_2$, b) **1**·**6**, c) oxaliplatin, d) CB[7]·oxaliplatin, and e) **1**·oxaliplatin.

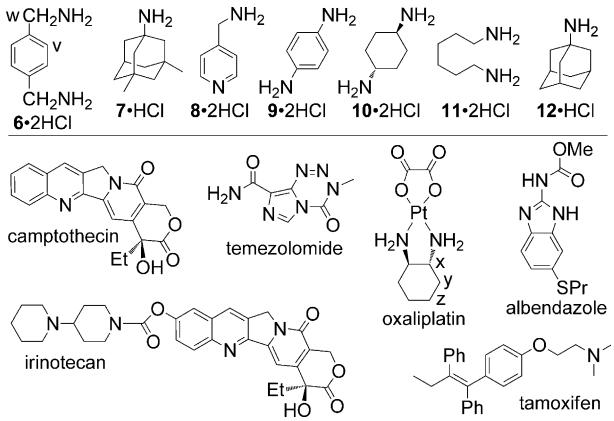

Figure 2. Chemical structures of guests **6**–**12** (top) and drugs (bottom) used in this study.

the presence of drug to form the **1**·drug complex. Before proceeding with the encapsulation of **1** with oxaliplatin we decided to study the binding strength of unfunctionalized CB[7] toward biotin. For this purpose we performed a ^{1}H NMR competition assay[3a,b] between **7** and biotin for CB[7] (the Supporting Information), which allowed us to determine the K_a value for CB[7]·biotin as $(7.0 \pm 1.3) \times 10^3\,\text{M}^{-1}$. In a related way we studied the ability of a series of guests of known affinity toward CB[7] with stepwise increasing the K_a value (**7**, $K_a = 2.5 \times 10^4\,\text{M}^{-1}$; **8**, $K_a = 3.6 \times 10^5\,\text{M}^{-1}$; **9**, $K_a = 2.1 \times 10^6\,\text{M}^{-1}$; **10**, $K_a = 2.3 \times 10^7\,\text{M}^{-1}$; **11**, $K_a = 9.0 \times 10^7\,\text{M}^{-1}$; **12**, $K_a = 4.2 \times 10^{12}\,\text{M}^{-1}$) to disrupt the $\mathbf{1}_2$ assembly (the Supporting Information) and found that guests with $K_a \geq 10^5\,\text{M}^{-1}$ form the monomeric **1**·guest complexes. The relatively low affinity of CB[7] toward biotin suggested that a wide variety of drugs could be encapsulated inside **1** for the purpose of targeted drug delivery. Figure 1 c–e shows the ^{1}H NMR spectra recorded for oxaliplatin, CB[7]·oxaliplatin, and **1**·oxaliplatin. Although the ^{1}H NMR spectrum of **1**·oxaliplatin is more complex and less interpretable than that of CB[7]·oxaliplatin—owing to the lack of symmetry of **1**·oxaliplatin—the close correspondence of the upfield shifts observed for oxaliplatin within the two complexes indicates that oxaliplatin is bound within the CB[7] sized cavity in both cases. To assess the generality of our approach, we performed similar binding studies of **1** toward five additional anticancer agents (e.g. albendazole, tamoxifen, camptothecin, irinotecan, temezolomide) and observed the formation of the **1**·drug complexes in each case (the Supporting Information).[10f,19]

After having established that CB[7] derivative **1** is capable of binding to oxaliplatin and several other chemotherapeutic agents, we decided to determine whether the biotin targeting ligand endows it with the ability to be taken up by cancer cell lines that overexpress biotin receptors. For this purpose, we selected the murine lymphocytic leukemia L1210 and its derived L1210FR cell lines, which express biotin receptors at low and high levels, respectively.[17] To monitor the binding and uptake of **1** into L1210 and L1210FR cells we used flow cytometry and confocal microscopy. Because **1** is not fluo-

rescent on its own, we prepared fluorescent adamantane derivative **13** by reaction of **14** with fluorescein isothiocyanate (Scheme 1). Adamantaneamine and its derivatives bind with extraordinary affinity toward CB[7] ($K_a \approx 10^{12}\,M^{-1}$)[3b], which ensures that the **1**·**13** complex is thermodynamically stable at the μM concentrations used in the flow cytometry measurements. Complex **1**·**13** is also kinetically stable ($k_{out} = 1.9 \times 10^{-5}\,s^{-1}$; half-life = 10.1 h, the Supporting Information) over the timescale of the confocal microscopy and flow cytometry experiments. Figure 3a shows the results of flow cytometry experiments performed with L1210 and L1210FR cells in combination with CB[7]·**13** and **1**·**13**. The solid and dashed lines (Figure 3a) show the fluorescence intensity distributions that were observed for L1210 cells ($n = 10000$) treated with **1**·**13** and L1210FR cells ($n = 10000$) treated with CB[7]·**13**, respectively. These distributions establish the background level of fluorescence intensity to be expected in the absence of biotin receptor mediated uptake. Significantly, when L1210FR cells were treated with **1**·**13** we observed that most cells exhibited approximately 10-fold higher fluorescence intensity (gray line, Figure 3a), which we attribute to biotin receptor mediated binding and/or uptake. To further demonstrate the biospecific nature of this biotin receptor mediated pathway, we performed competition experiments by adding free biotin to the cells in increasing doses, which significantly reduced binding and/or uptake of **1**·**13** (Figure 3b). To demonstrate targeted internalization of **1**·**13** after binding, we performed confocal microscopy experiments (Figure 4). When L1210FR cells were treated with **1**·**13** we observed cytoplasmic and vesicular staining (**1**·**13**, green in Figure 4a,c), which colocalizes in part with endosomes labeled with Dextran-Alexa Fluor 647 (red in Figure 4b,c). In contrast, nontargeted CB[7]·**13** is not internalized (Figure 4d,f) under identical conditions. Additional experiments performed using **1**·**13** at 4 °C showed only surface binding of **1**·**13**, which could be internalized by raising the temperature to 37 °C for 30 min (Figure S32 in the Supporting Information). After having demonstrated proof-of-principle for ligand-targeted uptake of CB[7] derivatives, we sought to expand the range of chemistry that could be used to attach such ligands beyond click chemistry[15] and amide bond formation demonstrated above. One common attachment for peptide targeting ligands (e.g. RDG peptides) is through nucleophilic attack of cysteine (e.g. thiolate) residues. To demonstrate this mode of conjugation (Scheme 1), we transformed **2** into the corresponding iodo CB[7] derivative in situ under Finkelstein conditions followed by treatment with glutathione under basic conditions to yield CB[7] tripeptide **15** in good yield (69 %).[20]

Finally, we decided to determine the effectiveness of targeted delivery of oxaliplatin as its **1**·oxaliplatin complex to L1210FR cells.[21] For this purpose, we quantified the change in cell viability of L1210FR cells in the presence of increasing concentrations of oxaliplatin, CB[7]·oxaliplatin, **1**·oxaliplatin,

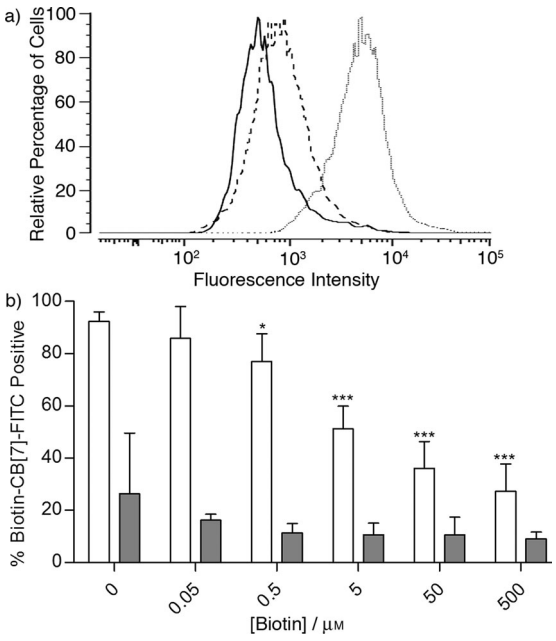

Figure 3. a) Murine lymphocytic leukemia cells overexpressing biotin receptors (L1210FR) and expressing normal levels of biotin receptors (L1210) showed target-specific binding of **1**·**13**. Solid (——) line: L1210 cells treated with **1**·**13** (2 μM); dashed line (-----): L1210FR cells treated with CB[7]·**13** (2 μM); gray line (——): L1210FR cells treated with **1**·**13** (2 μM). Uptake after 30 min was quantified with flow cytometry. The histograms are the fluorescence distribution of 10000 cells per condition and the experiment is representative of three independent repeats. b) Binding or uptake of **1**·**13** into L1210FR cells was inhibited by the presence of free biotin. L1210FR (white bars) and L1210 (gray bars) cells were incubated with biotin (0.05–500 μM) for 30 min, washed, and then incubated with **1**·**13** (2 μM) for 30 min. Cells were then collected for quantification with flow cytometry; 10000 cells per sample were analyzed. The average ($n = 4$) and standard deviation are shown. Unpaired t-test analysis was used for statistical analysis (*P = 0.01–0.05;**P = 0.001–0.01;***P = 0.001).

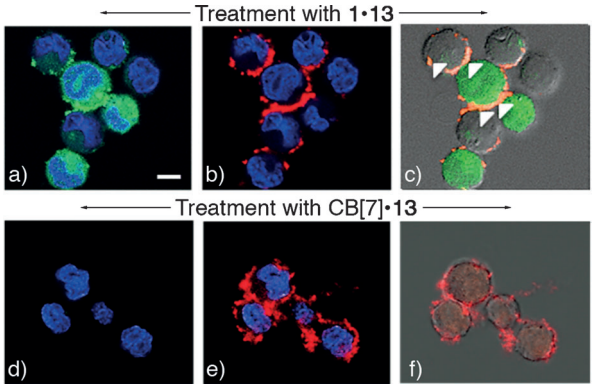

Figure 4. L1210FR cells that were incubated with **1**·**13** (15 μM, a–c) or CB[7]·**13** (15 μM, panels d–f) indicated receptor-specific uptake. L1210FR cells were treated with Dextran-Alexa Fluor 647 (125 μg mL^{-1}) overnight followed by **1**·**13** or CB[7]·**13** the next day. Color code: **1**·**13** or CB[7]·**13**, green; Hoechst 33342 (nuclear stain), blue; dextran labeled with Alexa Fluor 647 (lysosome/endosome stain), red. a,d) Blue and green channels for cells treated with **1**·**13** or CB[7]·**13**. b,e) Blue and red channels for cells treated with **1**·**13** or CB[7]·**13**, c,f) Overlay of brightfield image, green and red channels for cells treated with **1**·**13** or CB[7]·**13**. The white arrows highlight yellow regions of colocalization of **1**·**13** and Dextran-Alexa Fluor 647. Scale bar = 5 μm applies to all images.

and **5**·oxaliplatin by means of the MTS metabolic assay (Figure 5). Oxaliplatin (●) and CB[7]·oxaliplatin (○) exhibit very similar profiles of cellular toxicity (Figure 5), which further establishes[11] that oxaliplatin release from its CB[7] encapsulation complex does not greatly effect in vitro bioactivity. In contrast, the targeted complex **1**·oxaliplatin

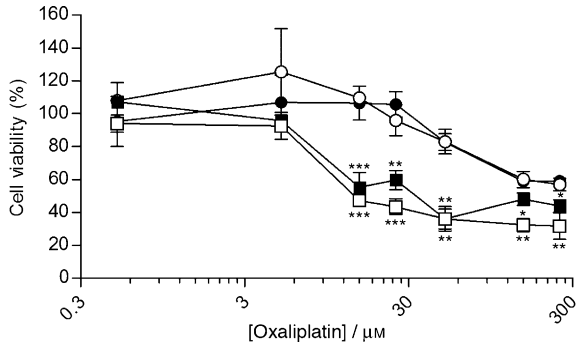

Figure 5. Container·drug complexes **1**·oxaliplatin and **5**·oxaliplatin result in target-specific decrease in cell viability in the biotin receptor positive murine lymphocytic leukemia cell line (L1210FR). Cells were incubated with oxaliplatin (●), CB[7]·oxaliplatin (○), **1**·oxaliplatin (■), or **5**·oxaliplatin (□) for 45 mins. Cells were then washed and incubated in fresh media for 24 h prior to MTS cell viability assay. Shown is the average ($n = 3$) and standard deviation of a representative experiment.

(Figure 5, ■) kills L1210FR cancer cells at significantly lower concentrations ($EC_{50} = 8$ μM) than CB[7]·oxaliplatin ($EC_{50} = 76$ μM) or oxaliplatin ($EC_{50} = 188$ μM) alone. To ascertain whether the short linker between the biotin ligand and the CB[7] cavity of **1** might sterically diminish the binding of **1**·oxaliplatin to the biotin receptor, we designed and tested the **5**·oxaliplatin complex the linker of which is extended by seven atoms. The cytotoxicity profile for **5**·oxaliplatin ($EC_{50} =$ 10 μM) is comparable to that of **1**·oxaliplatin (Figure 5), which establishes that the nature of the linking group is not having a deleterious effect on bioactivity. We also performed cell viability studies with L1210 cells, which do not overexpress biotin receptors (Figure S30 in the Supporting Information). CB[7]·oxaliplatin and **1**·oxaliplatin exhibit lower levels of cytotoxicity toward L1210 cells than oxaliplatin alone, probably because encapsulation decreases the concentration of free oxaliplatin.[11] The observation of enhanced cytotoxicity of **1**·oxaliplatin toward L1210FR cells, but reduced cytotoxicity toward L1210 cells provides further support for the targeted biotin-mediated uptake of **1**·oxaliplatin.

In summary, we have described the preparation of new monofunctionalized CB[7] derivatives, which permit conjugation reactions with targeting ligands by amide bond formation and thiolate S_N2 reactions. Biotin–CB[7] conjugate **1** maintains its ability to encapsulate a wide variety of anticancer agents (e.g. oxaliplatin) inside the CB[7] cavity. Further, we demonstrated by flow cytometry that biotin–CB[7] conjugate **1** is taken up in a biospecific receptor-mediated process by L1210FR cells. Finally, the targeted container·drug complex **1**·oxaliplatin was shown to exhibit approximately an order of magnitude higher bioactivity in in vitro MTS bioactivity assays with L1210FR cells. If these results can be translated to in vivo systems, then the reduction in cumulative oxaliplatin dose promises to reduce the incidence of peripheral neuropathy. The implications of the work extend beyond the system-specific details described above. For example, it is clear that the developed conjugation chemistry will allow the attachment of other targeting ligands (e.g. folate or RGD) and that the conjugates will encapsulate a range of chemotherapeutics, which promises new approaches toward cancer treatment. Similarly, attachment of CB[7] units to targeting antibodies can be envisioned, which would mitigate the bottleneck encountered during linker optimization[22] of therapeutic antibody drug conjugates. Finally, interaction of biotin–CB[7] conjugates (**1** and **5**) with avidin will deliver avidin·**1** complexes wherein the biotin binding sites have been morphed into high-affinity and stimuli-responsive CB[7] binding sites. These avidin·**1** complexes can be directly substituted into and thereby extend the scope of myriad avidin·biotin biotechnology applications. As such, we believe the prospects for the use of CB[7] molecular containers as key components of targeted chemotherapeutic agents and biotechnology applications is increasingly bright.

Received: June 12, 2013
Revised: August 2, 2013
Published online: September 13, 2013

Keywords: biotin · cucurbit[*n*]uril · drug delivery · host–guest chemistry · oxaliplatin

[1] a) W. Freeman, W. Mock, N. Shih, *J. Am. Chem. Soc.* **1981**, *103*, 7367 – 7368; b) J. Kim, I. S. Jung, S. Y. Kim, E. Lee, J. K. Kang, S. Sakamoto, K. Yamaguchi, K. Kim, *J. Am. Chem. Soc.* **2000**, *122*, 540 – 541; c) A. Day, A. Arnold, R. Blanch, B. Snushall, *J. Org. Chem.* **2001**, *66*, 8094 – 8100; d) A. I. Day, R. J. Blanch, A. P. Arnold, S. Lorenzo, G. R. Lewis, I. Dance, *Angew. Chem.* **2002**, *114*, 285 – 287; *Angew. Chem. Int. Ed.* **2002**, *41*, 275 – 277; e) S. Liu, P. Y. Zavalij, L. Isaacs, *J. Am. Chem. Soc.* **2005**, *127*, 16798 – 16799.

[2] For leading reviews, see: J. Lee, S. Samal, N. Selvapalam, K. Kim, *Acc. Chem. Res.* **2003**, *36*, 621 – 630; J. Lagona, P. Mukhopadhyay, S. Chakrabarti, L. Isaacs, *Angew. Chem.* **2005**, *117*, 4922 – 4949; *Angew. Chem. Int. Ed.* **2005**, *44*, 4844 – 4870; W. M. Nau, M. Florea, K. I. Assaf, *Isr. J. Chem.* **2011**, *51*, 559 – 577; E. Masson, X. Ling, R. Joseph, L. Kyeremeh-Mensah, X. Lu, *RSC Adv.* **2012**, *2*, 1213 – 1247.

[3] a) W. L. Mock, N.-Y. Shih, *J. Org. Chem.* **1986**, *51*, 4440 – 4446; b) S. Liu, C. Ruspic, P. Mukhopadhyay, S. Chakrabarti, P. Y. Zavalij, L. Isaacs, *J. Am. Chem. Soc.* **2005**, *127*, 15959 – 15967; c) M. V. Rekharsky, T. Mori, C. Yang, Y. H. Ko, N. Selvapalam, H. Kim, D. Sobransingh, A. E. Kaifer, S. Liu, L. Isaacs, W. Chen, S. Moghaddam, M. K. Gilson, K. Kim, Y. Inoue, *Proc. Natl. Acad. Sci. USA* **2007**, *104*, 20737 – 20742; d) F. Biedermann, V. D. Uzunova, O. A. Scherman, W. M. Nau, A. De Simone, *J. Am. Chem. Soc.* **2012**, *134*, 15318 – 15323.

[4] C. Marquez, W. M. Nau, *Angew. Chem.* **2001**, *113*, 4515 – 4518; *Angew. Chem. Int. Ed.* **2001**, *40*, 4387 – 4390.

[5] W. L. Mock, J. Pierpont, *J. Chem. Soc. Chem. Commun.* **1990**, 1509 – 1511; I. Ghosh, W. M. Nau, *Adv. Drug Delivery Rev.* **2012**, *64*, 764 – 783.

[6] a) Y. H. Ko, E. Kim, I. Hwang, K. Kim, *Chem. Commun.* **2007**, 1305 – 1315; b) K. Moon, J. Grindstaff, D. Sobransingh, A. E.

Kaifer, *Angew. Chem.* **2004**, *116*, 5612 – 5615; *Angew. Chem. Int. Ed.* **2004**, *43*, 5496 – 5499; c) A. R. Urbach, V. Ramalingam, *Isr. J. Chem.* **2011**, *51*, 664 – 678; d) D. Das, O. A. Scherman, *Isr. J. Chem.* **2011**, *51*, 537 – 550; e) J. F. Young, H. D. Nguyen, L. Yang, J. Huskens, P. Jonkheijm, L. Brunsveld, *ChemBioChem* **2009**, *11*, 180 – 183; f) W.-H. Huang, S. Liu, P. Y. Zavalij, L. Isaacs, *J. Am. Chem. Soc.* **2006**, *128*, 14744 – 14745; g) J. B. Wittenberg, P. Y. Zavalij, L. Isaacs, *Angew. Chem.* **2013**, *125*, 3778 – 3782; *Angew. Chem. Int. Ed.* **2013**, *52*, 3690 – 3694.

[7] A. Hennig, H. Bakirci, W. M. Nau, *Nat. Methods* **2007**, *4*, 629 – 632; T. Minami, N. A. Esipenko, B. Zhang, M. E. Kozelkova, L. Isaacs, R. Nishiyabu, Y. Kubo, P. Anzenbacher, *J. Am. Chem. Soc.* **2012**, *134*, 20021 – 20024.

[8] E. A. Appel, J. del Barrio, X. J. Loh, O. A. Scherman, *Chem. Soc. Rev.* **2012**, *41*, 6195 – 6214.

[9] C. Klöck, R. N. Dsouza, W. M. Nau, *Org. Lett.* **2009**, *11*, 2595 – 2598; X. Lu, E. Masson, *Org. Lett.* **2010**, *12*, 2310 – 2313.

[10] a) E. Kim, D. Kim, H. Jung, J. Lee, S. Pail, N. Selvapalam, Y. Yang, N. Lim, C. G. Park, K. Kim, *Angew. Chem.* **2010**, *122*, 4507 – 4510; *Angew. Chem. Int. Ed.* **2010**, *49*, 4405 – 4408; b) V. D. Uzunova, C. Cullinane, K. Brix, W. M. Nau, A. I. Day, *Org. Biomol. Chem.* **2010**, *8*, 2037 – 2042; c) S. Walker, R. Oun, F. J. McInnes, N. J. Wheate, *Isr. J. Chem.* **2011**, *51*, 616 – 624; d) J. Zhang, R. J. Coulston, S. T. Jones, J. Geng, O. A. Scherman, C. Abell, *Science* **2012**, *335*, 690 – 694; e) D. Ma, G. Hettiarachchi, D. Nguyen, B. Zhang, J. B. Wittenberg, P. Y. Zavalij, V. Briken, L. Isaacs, *Nat. Chem.* **2012**, *4*, 503 – 510; f) E. A. Appel, M. J. Rowland, X. J. Loh, R. M. Heywood, C. Watts, O. A. Scherman, *Chem. Commun.* **2012**, *48*, 9843 – 9845.

[11] Kim and co-workers have used perhydroxylated CB[6] as a building block to prepare 70 nm polymer nanocapsules. When noncovalently decorated with spermine-targeting ligand conjugates, these CB[6] polymer nanocapsules are internalized into HepG2 cells and release encapsulated drugs or fluorophores. See Ref. [10a] and K.-M. Park, D.-W. Lee, B. Sarkar, H. Jung, J. Kim, Y. H. Ko, K. E. Lee, H. Jeon, K. Kim, *Small* **2010**, *6*, 1430 – 1441.

[12] C. Yang, H. Z. Liu, X. F. Zhong, W. D. Lu, *BMC Biotechnol.* **2011**, *11*, 21; T. Alcindor, N. Beauger, *Current Oncology* **2011**, *18*, 1; L. M. Pasetto, M. R. D'Andrea, E. Rossi, S. Monfardini, *Crit. Rev. Oncol. Hematol.* **2006**, *59*, 159 – 168.

[13] Y.-J. Jeon, S.-Y. Kim, Y. H. Ko, S. Sakamoto, K. Yamaguchi, K. Kim, *Org. Biomol. Chem.* **2005**, *3*, 2122 – 2125; N. J. Wheate, A. I. Day, R. Blanch, A. Arnold, C. Cullinane, J. G. Collins, *Chem. Commun.* **2004**, 1424 – 1425; N. J. Wheate, D. P. Buck, A. I. Day, J. G. Collins, *Dalton Trans.* **2006**, 451 – 458.

[14] P. S. Low, W. A. Henne, D. D. Doorneweerd, *Acc. Chem. Res.* **2008**, *41*, 120 – 129; R. A. Petros, J. M. DeSimone, *Nat. Rev. Drug Discovery* **2010**, *9*, 615 – 627; W. Arap, R. Pasqualini, E. Ruoslahti, *Science* **1998**, *279*, 377 – 380.

[15] a) D. Lucas, T. Minami, G. Iannuzzi, L. Cao, J. B. Wittenberg, P. Anzenbacher, Jr., L. Isaacs, *J. Am. Chem. Soc.* **2011**, *133*, 17966 – 17976; b) N. Zhao, G. O. Lloyd, O. A. Scherman, *Chem. Commun.* **2012**, *48*, 3070 – 3072; c) L. Cao, L. Isaacs, *Org. Lett.* **2012**, *14*, 3072 – 3075; d) B. Vinciguerra, L. Cao, J. R. Cannon, P. Y. Zavalij, C. Fenselau, L. Isaacs, *J. Am. Chem. Soc.* **2012**, *134*, 13133 – 13140; e) Y. Ahn, Y. Jang, N. Selvapalam, G. Yun, K. Kim, *Angew. Chem.* **2013**, *125*, 3222 – 3226; *Angew. Chem. Int. Ed.* **2013**, *52*, 3140 – 3144.

[16] The high values of K_a and slow kinetics of dissociation typically observed for CB[7]·guest complex make them particularly well suited for development as targeted therapeutics, since these properties will prevent premature release.

[17] We thank Prof. Ojima for providing the L1210 and L1210FR cell lines. See also, I. Ojima, *Acc. Chem. Res.* **2008**, *41*, 108 – 119.

[18] Y. Cohen, L. Avram, L. Frish, *Angew. Chem.* **2005**, *117*, 524 – 560; *Angew. Chem. Int. Ed.* **2005**, *44*, 520 – 544.

[19] Y. Zhao, D. P. Buck, D. L. Morris, M. H. Pourgholami, A. I. Day, J. G. Collins, *Org. Biomol. Chem.* **2008**, *6*, 4509 – 4515; A. L. Koner, N. Dong, S.-F. Xue, Q.-J. Zhu, Z. Tao, Y. Zhao, L.-X. Yang, *Supramol. Chem.* **2008**, *20*, 659 – 665.

[20] We have also synthesized a CB[7]–RGD conjugate (**16**) by the reaction of iodo CB[7] with cyclo(-Arg-Gly-Asp-D-Phe-Cys), as detailed in the Supporting Information.

[21] Many targeted drug delivery systems take advantage of the enhanced permeability and retention (EPR) effect, which is operative for systems larger than approximately 40 kD. The molecular weight of **1** is 1474 and therefore we do not expect **1**·drug complexes to benefit from the EPR effect. See: H. Maeda, *Bioconjugate Chem.* **2010**, *21*, 797 – 802.

[22] B. Hughes, *Nat. Rev. Drug Discovery* **2010**, *9*, 665 – 667.

